

REPORT OF GROUP VIIIPOSSIBILITIES AND LIMITATIONS OF DETECTORS AND DATA HANDLING

Convenor : D. R. Nygren

M. Breidenbach, G. Charpak, B. Dolgoshein, T. Ekelöf, I. Golotvin, K. Lanius, Y. Prokoshkin, F. Sauli, Y. Watase, W. J. Willis, and P. Zanella.

1. INTRODUCTION

The work of this group was divided into the following four general topics:

- i) open problems in particle identification;
- ii) limits in spatial and time resolution;
- iii) energy flow;
- iv) new data acquisition architectures.

In addition, various members of this group had extensive involvement with the work of groups V, VI, and VII. A comprehensive study of the very extensive range of possible developments within these topics was not attempted, but a consensus was reached that

- i) the physics programs anticipated for both fixed target and colliding beam facilities can largely be accomplished by reasonable extrapolation of present techniques;
- ii) higher energies will permit some new techniques to be employed;
- iii) significant effort may be necessary to realize some potentially useful ideas or techniques, but would be an excellent investment for the advancement of the field.

2. OPEN PROBLEMS IN PARTICLE IDENTIFICATION

The  $\gamma$  range of possible interest for hadron identification is very wide. In electron-positron collisions at  $\sqrt{s} = 700$  GeV the range is  $10 \lesssim \gamma \lesssim 10^3$ , and for the physics anticipated with 20 TeV protons the range is  $10^2 \lesssim \gamma \lesssim 10^5$ . We address first the problem for electron-positron collisions.

2.1 Particle identification for electron-positron colliders

Extrapolation of current data<sup>1)</sup> suggests charged particle multiplicities of  $\sim 50$ , and a very pronounced jet structure. It was recognized that the distribution of flavor within these high multiplicity events may not provide much recoverable information due to combinatorial problems or may simply reflect statistical aspects of well understood dynamical mechanisms. Nevertheless, we decided to pursue the task of leading hadron identification on the basis that detailed information about these events is likely to be valuable in ways that cannot now be foreseen.

We decided to concentrate on the Cerenkov ring imaging technique, as the possibilities for development from the present state seem particularly promising. The success of the technique depends not only upon the detection with high spatial accuracy of a sufficient number of Cerenkov photons for efficient ring image recognition in an overlapping and crowded situation, but also on the existence of a practical Cerenkov radiator. The attractiveness of a full solid angle Cerenkov detector for the electron-positron environment depends sensitively on the radiator length, especially since a crude momentum measurement is vital to make mass identification.

Choosing the parameters of the detector to match the electron-positron collider environment places some required performance characteristics beyond present state of the art. The configuration under evaluation was taken as follows:

- i) UV-sensitive MWPC's for photon detection and coordinate measurement, as proposed by Ypsilantis and Seguinot.<sup>2)</sup> (Other schemes involving microchannel plate photomultipliers might be considered but are more futuristic.)
- ii) Spatial resolution of the photon detector  $\sigma_x = 0.15$  mm rms. This resolution, along with chromatic and other aberrations, multiple scattering, etc. determines the resolution  $\Delta\gamma$ .
- iii)  $\Delta\gamma/\gamma_{\text{MAX}} = 0.3$ . This gives three standard deviations in  $\pi/K$  separation and two for  $K/p$ .
- iv) Number of detector photoelectrons  $N_\gamma = 8$ . This value was selected as a practical minimum needed for efficient pattern recognition.
- v) Radiator length  $L = 1.5$  metres. This modest length nonetheless implies a spherical detector volume of 6 m diameter.<sup>3)</sup>
- vi) Quality parameter  $N_0 = 80$  photons/cm. This value is more than twice that achieved currently.

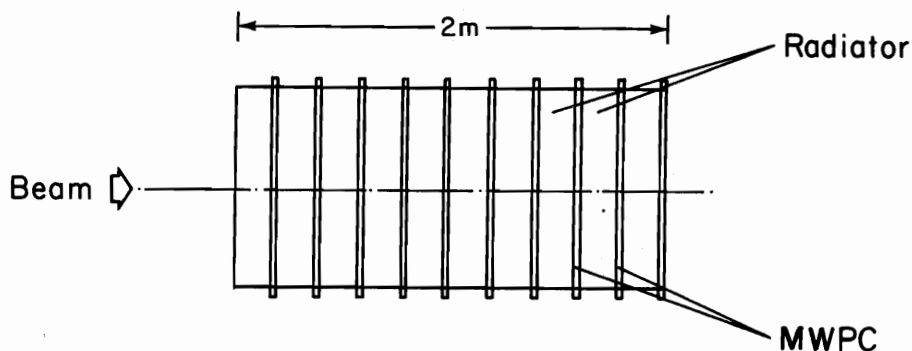
The report by Ekelöf in these proceedings addresses the possibilities and limitations of this technique in quantitative detail. There the conclusion is reached that it may be possible to construct a successful detector of very large solid angle using an argon gas radiator of 1.5 m length at 1 atmosphere. For this to be realizable however, large area, efficient, high-resolution, position-sensitive detectors for photons 6.5-7.5 eV must be developed. With these performance specifications the device is in principle capable of providing  $\pi/K$  separation up to 115 GeV.

## 2.2 Fixed target detectors in the 20 TeV environment

Since the interesting laboratory solid angle is so much less than the electron-positron collider requirements, the radiator length may be increased substantially. Only helium is an attractive radiator candidate and Ekelöf concludes that an atmospheric pressure radiator of 13.3 m length can

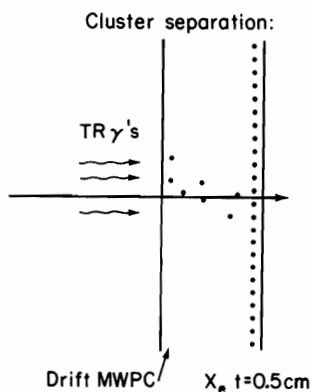
provide, with similar assumptions for technical performance, full  $\pi/K/p$  separation up to about 585 GeV. For the very forward or secondary beam application, the spot-focusing techniques as developed by Meunier et al. are certain to be valuable as chromatic aberration and position resolution requirements can be relaxed.<sup>4)</sup>

Above  $\gamma$  values of 500,  $K/\pi$  separation may be accomplished by a very compact TR detector, perhaps even as small as two metres in length. A particular configuration was studied by Dolgoshein et al. and is reproduced in Fig. 1. The particles to be identified impinge upon a linear array of 10 modules. Each module is composed of  $2 \times 10^3$  Li foil radiators (thickness  $10\mu\text{m}$ , gap  $100\mu\text{m}$ ) followed by a xenon-filled MWPC, whose characteristics are depicted in Fig. 2. The xenon MWPC's are constructed to provide both photon counting capability and photon energy measurement.



XBL 803-6840

Fig. 1. View of TR detector for  $K/\pi$  separation. Modules are composed of  $2 \times 10^3$  Li foil radiators followed by xenon-filled MWPC capable of photon counting and photon energy measurements.



XBL 803-6841

Fig. 2. Cross section of xenon-filled MWPC. Ionization clusters from conversion of TR are drifted to anodes. Drift-time differences allow individual photon energy measurements.

The TR photons are converted by the xenon, forming a halo surrounding the particle trajectory. The resultant clusters of ionization are also distributed in depth, according to the attenuation lengths in xenon of the parent photons. The asymmetric construction allows both a weak drift field and a large gain on the anodes, so that the energies and times-of-arrival of the various clusters may be clearly distinguished. At the same time, the unwanted ionization deposited by the particle itself may be suppressed by an energy threshold of a few keV. The few  $\delta$ -rays exceeding this energy threshold do not compromise the  $K/\pi$  separation significantly. The actual  $K/\pi$  separation is accomplished by a threshold requirement in  $N_\gamma$ , the total number of detected photons in all of the MWPC's.

A quantitative Monte Carlo study of this configuration has been made for two different incident momenta, 83.7 GeV/c ( $\gamma_\pi = 600$ ) and 195.4 GeV/c ( $\gamma_\pi = 1400$ ). In each case, an equal number of kaons and pions are employed, and the detected photon energy threshold was taken to be 3.0 keV. The results for  $N_\gamma$ , the number of  $\delta$ -rays  $N_\delta$  exceeding this threshold, and the resultant total are given in Table 1.

Table 1

Detected Ionization From TR and  $\delta$ -rays Per Track

$\gamma$		$N_\gamma$		$N_\delta$	$N_{TOTAL}$	
Pion	Kaon	Pion	Kaon	$\pi$ or K	Pion	Kaon
600	170	15.9	0.6	1.2	17.1	1.8
1400	395	36.2	8.6	1.2	37.8	9.8

The average number of measured photons from pions due to TR is substantial, giving very high detection efficiency. That the separation is also very good can be seen from the  $N_\gamma$  spectra in Fig. 3. It would be valuable to extend these studies to much higher  $\gamma$  values and to establish maximum feasible counting rates.

What is the practical maximum  $\gamma$  value for which  $\pi/K$  separation can be made with TR? There is considerable information in the energy and angular distributions of TR. This is an area in which further effort would be fruitful, as would more detailed comparisons with Cerenkov ring imaging techniques.

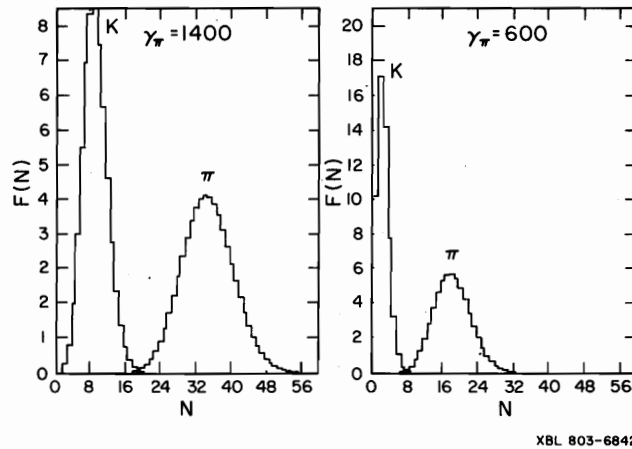


Fig. 3. Distribution of  $N_{TOTAL}$ , the number of converted TR photons and  $\delta$ -rays above 3.0 keV energy threshold for two momenta. Pions and kaons are well separated.

### 2.3 General comments

At the very highest  $\gamma$  values, synchrotron radiation (SR) for particles other than electrons may be of interest. The possibility of using a wiggler geometry for hadron identification was examined, but ultimately found wanting in photon flux. It may be interesting to explore further possibilities in the interference effects between Cerenkov and synchrotron (wiggler) radiation. Readers are also encouraged to read the stimulating report by Willis in the Proceedings of the previous ICFA Workshop, held at Fermilab.

At the other  $\gamma$  extreme, it is worth noting that typical particle energies are very low for electron-positron annihilation collisions even at  $\sqrt{s} = 700$  GeV. If the actual charged multiplicity is given correctly by extrapolation of current trends ( $N_{CH} \approx 50$ , as mentioned earlier) the typical energy is only about 10 GeV. In this high particle density "jet" regime, the use of ionization density in gases, or "dE/dx", for particle identification may be competitive or even superior since the information is concentrated within the track itself. Recent experimental results for the  $\gamma$  dependence of ionization in a xenon-hydrocarbon mixture are given in Fig. 4.<sup>5)</sup> The data emphasize the crucial role of the density effect. Further work is needed to establish optimal choices for gas composition, pressure, ionization sampling and data treatment, and is strongly encouraged. If techniques are developed for measuring primary ionization, such as the time expansion chamber of Walenta, then the dE/dx method will become even more attractive.

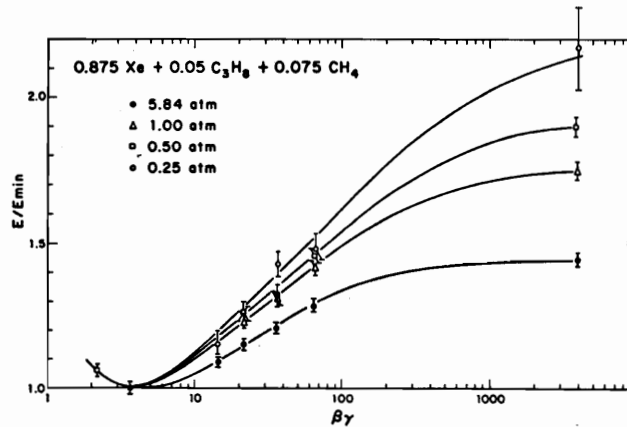


Fig. 4. The most probably energy loss as a function of  $\beta\gamma$  normalized to its minimum value ( $\beta\gamma \approx 3.5$ ) for a particular xenon-hydrocarbon mixture sample of 2.3 cm length. The variation of the density effect is clearly evident for the different pressures.

Lepton identification was not studied as a separate topic as this problem is generally made easier by the higher energies, and just two remarks will be added. It may be useful to exploit the "anomalous" energy loss of multi-TeV muons in  $H_1-Z$  materials for this purpose, thereby avoiding the necessity to absorb all hadrons as a means of muon identification. At electron-positron colliders, high magnetic field spectrometers will cause secondary electrons to radiate several SR photons. As they convert in nearby gas these photons will create an outboard halo for the electron track, and can be used to identify electrons.

### 3. LIMITS IN SPATIAL AND TIME RESOLUTION

#### 3.1 Gaseous detectors

The processes which limit spatial resolution in gaseous detectors are now thought to be generally well understood. These factors and the current state-of-the art have been reviewed by Chrapak in the proceedings of the previous workshop, and also by Sauli<sup>7)</sup>. Broadly speaking, the spatial resolution is affected by three distinct processes:

- i) Delta rays produced along the particle trajectory, leading to an intrinsic "size" for the residual track;
- ii) Diffusion of the ionization electrons during the time interval between generation and measurement;
- iii) Measurement techniques, which almost invariably involve electron multiplication by avalanche mechanisms.

However, the present state-of-the art resolution does not represent a fundamental limit because in some circumstances pressurization of the gas can provide a substantial improvement. To understand the effects that pressurization can introduce, we first examine the probability for creation of  $\delta$  rays of a certain range or greater by a high energy particle traversing a specified sampling interval. This relationship for two pressures and two sampling intervals of typical interest is illustrated in Fig. 5<sup>7)</sup>.

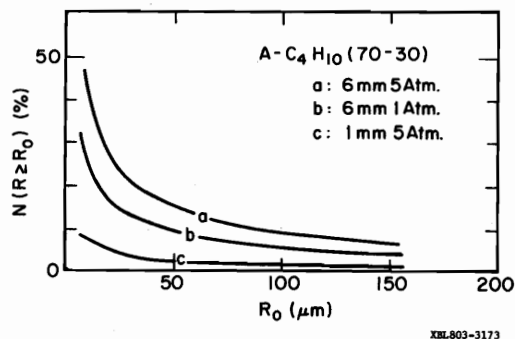


Fig. 5. Probability of obtaining a  $\delta$ -electron with a range equal to or greater than  $R_0$ , in the detection of minimum ionizing tracks in the indicated gas mixture and conditions.

The main point of Fig. 5 is that advantage of pressure is realized only by the combination of increased pressure and reduced sampling length. A crude rule of thumb might be that pressure and sampling interval should be scaled to maintain constant average ionization per sample. This behavior is directly related to the skewed characteristic of the Landau distribution, and is of course the same phenomenon that leads to the requirement of extensive sampling for particle identification by ionization measurement.

While the behavior of  $\delta$ -ray range with pressure and sampling length is not completely simple, the diffusion of the electrons in the absence of fields is expected to follow an inverse square root dependence (until multi-body effects enter at ultra high pressures). The introduction of magnetic and/or electric drift fields leads to considerable theoretical complication but for most practical gas mixtures the behavior can be understood well enough in terms of a few averaged quantities such as electron temperature, mean free path, and inelasticity of electron-molecule collisions<sup>8,9</sup>). In particular, the inverse square root dependence of diffusion with pressure holds if the ratio of electric drift field to the gas density  $E/N$  is held constant. It is also useful to remember that the electron drift velocity is independent of pressure if  $E/N$  is held constant.

Therefore, the consequences of pressurization can be substantial reductions in the effects of  $\delta$ -rays and electron diffusion. In many experimental arrangements, the price of containment may be too high, but already large-scale pressurized drift chambers are part of the PEP and PETRA experimental programs, and at Fermilab a very high pressure streamer chamber (25 atm.) has been in use for the determination of charmed lifetimes.

Ideally, for gaseous detectors involving proportional amplification near anode wires it would be desirable to scale the anode wire diameter inversely with pressure, so that the same multiplication would be obtained

at constant anode voltage. While pressure can be scaled up more than a factor of 100, it is unfortunately not practical to consider wire diameters more than a factor of two or three smaller than in current use. If the anode diameter is left constant as pressure is scaled up, there are two unpleasant and significant effects:

- i) The anode voltage must increase substantially, approximately as  $P^{1/2}$ ;
- ii) The electrical signals derived from the motion of positive ions away from the avalanche region at the anode are much slower, owing to the reduced velocity of these ions.

We now describe two examples which will illustrate some of the possibilities available through pressurization.

The first example addresses the need to detect and study the production of new flavor states. This problem was discussed extensively in the previous Workshop proceedings in the reports by Lanius and by Fischer and Sandweiss. In brief, the experimental challenge is to satisfy the following requirements:

- i) Vertex resolving power sufficient to distinguish primary production and secondary decay vertices in a majority of cases;
- ii) Rate and triggering capability sufficient to accommodate the tiny cross-sections expected for the events of interest.

Ground states involving charm and bottom quarks are expected to have mean lifetimes in the range  $10^{-13}$  to  $10^{-14}$  sec. As shown in the previous Workshop reports this translates into spatial resolution requirements in the vertex region of  $\Delta x, \Delta z \lesssim 10 \mu\text{m}$  and track pair resolution of not more than  $100 \mu\text{m}$ .

To satisfy these requirements, a small drift chamber filled with up to 500 (!) atmospheres of helium is proposed, as illustrated in Fig. 6<sup>10</sup>.

Its main characteristics are as follows:

- i) A gaseous He target with a density of  $0.1 \text{ g/cm}^3$  and acting at the same time as a drift chamber;
- ii) The contribution to spatial resolution caused by electron diffusion over the dimensions indicated is only  $\sim 10 \mu\text{m}$ ;
- iii) Measurement of drift times by scintillation light produced at anodes rather than by electrical signals from avalanche multiplication;
- iv) A vertex transverse coordinate resolution of  $\Delta x \approx 4\text{-}5 \mu\text{m}$  (obtained by Monte Carlo methods for vertex fit of extrapolated secondary tracks, limited by electron diffusion and multiple Coulomb scattering);
- v) A vertex longitudinal coordinate resolution of  $\Delta Z \approx 100 \mu\text{m}$  at 400 GeV (again obtained by Monte Carlo from vertex fit of extrapolated secondaries);
- vi) A two-track resolving power of  $\sim 100 \mu\text{m}$ ;
- vii) Rates up to  $10^6 \text{ sec}^{-1}$  can be accepted.
- viii) A self-triggering mode is possible.

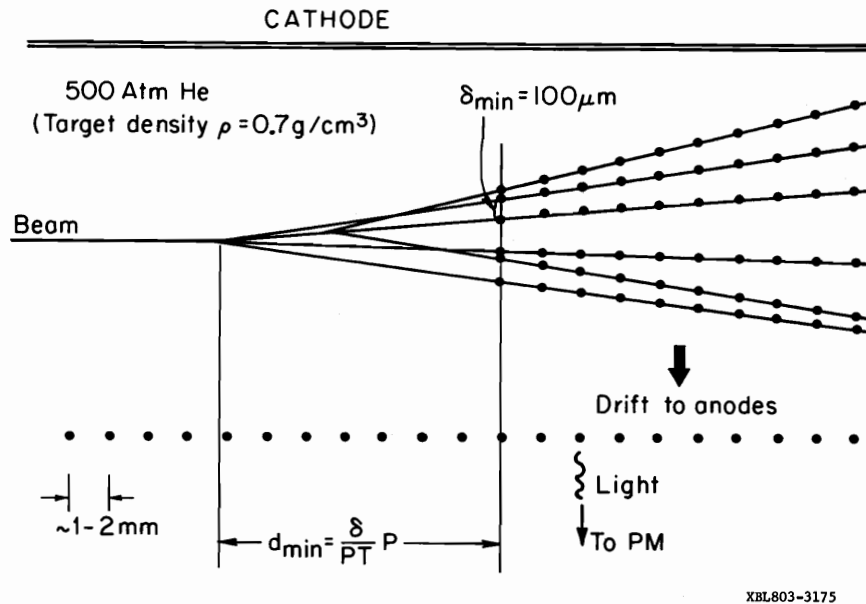


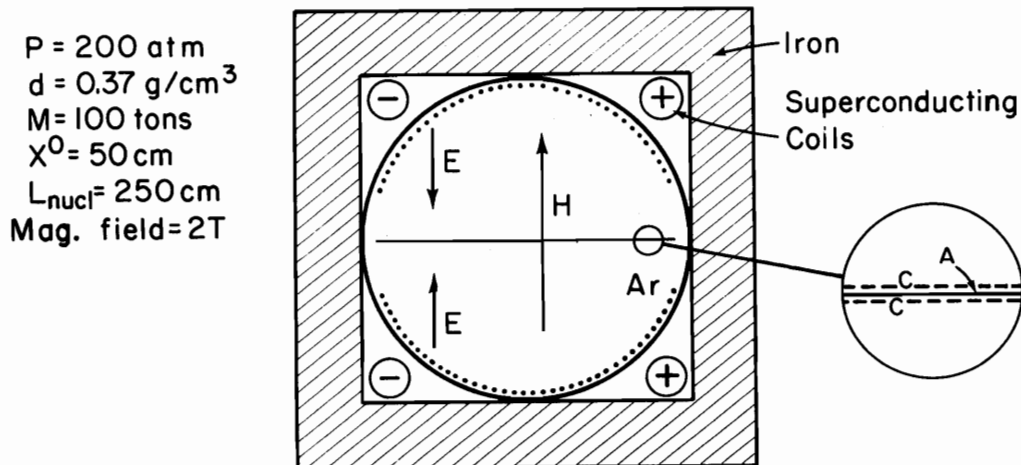
Fig. 6. High-pressure drift chamber for the detection of short-lived states. Detection is mediated by production of scintillation light rather than amplification of ionization in order to increase rate capability

The advantages obtained by using the helium scintillation light for drift time measurement are twofold. First, the anodes can be operated to produce little or no additional ionization, thereby reducing or eliminating electric drift field distortion due to positive ion space charge. Second, the scintillation light is generated much more rapidly than the electrical signals could be, as the scintillation occurs mainly during the very rapid collection of primary drift electrons close to the anodes. Both of these effects increase the rate capability. The Monte Carlo results for production of these short-lived states lead the authors to conclude that the primary and secondary decay vertices will be resolved in a majority of cases.

Much more work has been done than can be described here, but it is essential that these studies be extended to the multi-TeV regime. It may be valuable to compare the problems of high pressure gas containment and window fabrication to the cryogenic problems of the corresponding detector operated with liquid helium, assuming that suitable drift and scintillation can be obtained.

The second high pressure example is intended for the study of neutrino interactions and is at the other extreme of the physical scale (see Fig. 7)<sup>10)</sup>. Briefly, the detector envisaged for multi-TeV neutrino physics is contained within a large cylindrical pressure vessel perhaps two meters in diameter and 80 meters in length along the beam direction. The vessel is embedded in a transverse magnetic field of perhaps 2T and is filled with a predominantly argon gas mixture to a pressure of 200 atm. Data recording is accomplished by conventional proportional wire planes located in the vessel midplane (20  $\mu\text{m}$  diameter anodes, 5 mm spacing, wire direction perpendicular to the beam direction). The midplane is oriented so that its normal direction is parallel to the magnetic field. Electrostatic structures are provided to produce a uniform drift field (similar to ISIS geometry). Ionization electrons generated on either side of the anode plane by neutrino interactions in the gas volume are drifted toward the anode and multiplied several thousand times, so that no exotic electronic requirements are involved. Transverse coordinates are determined by drift time and current division, and the pulse height information allows all but the shortest nuclear fragments to be identified. The efficiency for separating  $\nu$ -N from  $\nu$ -e events is expected to be good. The gas has a radiation and interaction length of 50 cm and 250 cm respectively, and represents a total mass of  $\approx 100$  tons.

Experimental work has been done on the relevant properties of some gas mixtures appropriate for this scenario. The gas mixtures studied were argon-xenon with varying fractions of argon and  $\text{CH}_4$ . The xenon concentration was held fixed at 0.5% for all mixtures, and  $\text{CH}_4$  was varied from 0.0

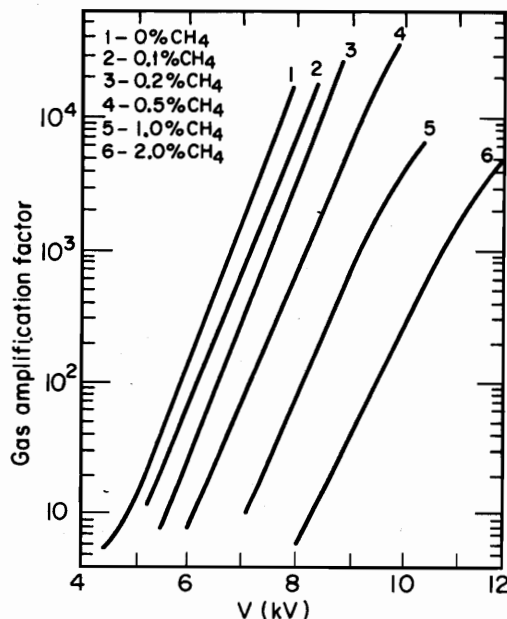


XBL 803-6843

Fig. 7. Multi-TeV neutrino detector filled with high pressure argon gas. The length of the detector along the beam is  $\approx 80$  metres.

to 2.0%. The pressure was varied up to 175 atm. and the anode wire diameter of the test chamber was 20  $\mu\text{m}$ . It is amusing to scale the test geometry to atmospheric pressure in which case the anode wire diameter would be 2 mm! Remarkably, rather high gain is possible, and values in excess of  $10^4$  for several mixtures have been achieved (see Fig. 8). The small amount of xenon acts to reduce substantially the high voltage needed to reach a particular gain, probably through a high density Penning effect. The electron drift velocities were also measured, giving the expected behavior and a typical value of 1 cm/ $\mu\text{sec}$  at fields of 1.5 kV/cm. Electron diffusion during drift was also measured and found to behave as expected, so the spatial resolution is expected to be comparable to that of large bubble chambers. Also, such large pressure vessels are not uncommon in industrial applications, but electrical feedthroughs may require development.

Pressurized drift chambers under test conditions (e.g., Moscow and Heidelberg) have already given  $\approx 25$  micron resolution. Translating this performance into large-scale apparatus will not obviously become easier with time, and it seems likely that the ultimate limit may in practice lie in ordinary causes like fabrication and calibration errors, long-term deformations due to strain relief, vibration, temperature and pressure cycling, etc., and needless to say, excessive costs.



XBL803-3174

Fig. 8. Gas amplification factor in argon-xenon as a function of anode voltage for various admixtures of CH<sub>4</sub>. Pressure is 100 atmospheres, anode wire diameter is 20  $\mu\text{m}$ .

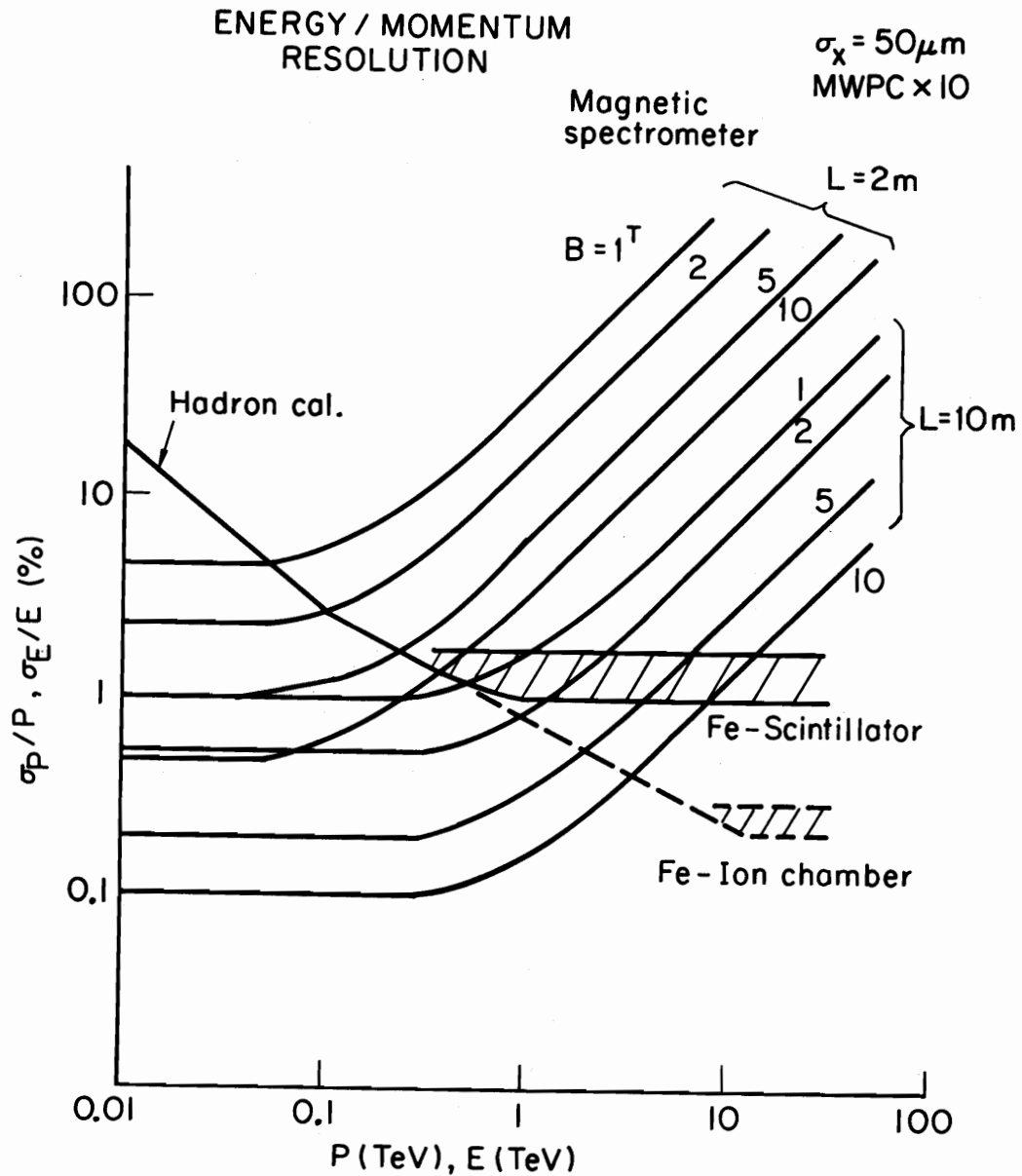


Fig. 9. Comparison of extrapolated performance for calorimeters and magnetic spectrometers. Limitations due to system stability and calibration are suggested for two calorimeter techniques.

### 3.2 Spatial resolution developments in non-gaseous detectors

Here we limit ourselves to developments not discussed in the previous Workshop proceedings or to those cases for which some new results may be available, but we do not wish to imply that omitted techniques are uninteresting.

#### 3.2.1 Liquid argon ionization chamber

A Berlin - CERN - Munich Collaboration has constructed and tested a small test detector arranged as a telescope of four chambers with parallel metallized glass electrodes<sup>12)</sup>. The collecting electrodes (anodes) of the chambers consisted of 19 chromium or gold strips, each 10 mm wide and separated by 20  $\mu\text{m}$  centre-to-centre. The active area of the chamber was  $0.4 \times 3 \text{ mm}^2$ . Each strip was connected to an individual electronic channel containing a charge-sensitive preamplifier, pulse-shaping amplifier and ADC. In the off-line analysis, a hit was accepted if the signal exceeded the pedestal by at least four standard deviations of the pedestal width. The weighted mean of the hits defined the coordinate in each plane. Straight line fits and residuals were computed if at least three chambers had hits. For a chamber depth of 2 mm the rms measuring error of a single chamber is  $8.4 \pm 0.5 \mu\text{m}$  and the two point resolution is in the order of 50  $\mu\text{m}$  at 100% efficiency. A reduction of the chamber depth gives improved resolution. Operated as a vertex detector, it would have an advantage in sensitivity of about three orders of magnitude compared with a rapid cycling bubble chamber. Rates possibly up to  $10^7/\text{sec}$  may be tolerated, but a large array of extremely low noise electronics is required. Large scale integrated circuit technology is needed here to bring this technique to a practical state.

#### 3.2.2 Noble liquid drift chambers

The principal advantage of using the drift principle in liquids is the reduction of the number of electronics channels by two orders of magnitude when compared with the strip hodoscope technique discussed just above. The disadvantage is at least an order of magnitude reduction in tolerable beam intensity. Diffusion is very small, allowing in principle very accurate measurements over drift distances of several centimetres.

Miyajima et al.<sup>13)</sup> have reported on measurements with a liquid xenon drift chamber. They achieved a stable amplification of 200, allowing considerable simplification in the electronics. They quote an rms measuring error of  $\approx 20 \mu\text{m}$  and expect that 10  $\mu\text{m}$  can be achieved. The subject of purification, electron drift and amplification in liquids deserves more effort and could be very fruitful.

#### 3.2.3 Semiconductors

The use of solid-state techniques in high energy physics appears to be remarkably under-developed, but the situation could change with

developmental work. There are fundamental questions regarding how much radiation damage can be tolerated, and the answers will depend substantially on the technology of implementation. Already, Radeka and Fischer at BNL found that minimum ionizing particles could be observed in a commercial CCD device, a TV camera<sup>14)</sup>. Such two-dimensional imaging devices could be very attractive if readout techniques which avoid the time-consuming raster scan are developed. Radeka et al. have also developed an ingenious segmented charge division technique of converting charge ratios to time differences. The method promises to give 10  $\mu\text{m}$  resolution with channels distributed at 0.5 mm intervals, and can be adapted to large area configurations<sup>14)</sup>.

### 3.3 Time resolution

A promising technique using secondary emission from a cathode in vacuum offers in principle the prospect of both subnanosecond time resolution and excellent spatial resolution. Microchannel plate phototubes also display time resolution better than 100 psec, and can be fabricated in multianode versions suitable for Cerenkov imaging. There is apparently an antagonistic relationship in the chemistries of the photocathode and multiplier plates, and lifetimes for the presently available tubes have not been satisfactory. The narrow-gap spark counter developed by Pestov has demonstrated a resolution of 28 psec.

Nevertheless, we do not foresee across-the-board prospects for dramatic improvements in time resolution. Coincidence circuits based on leading edge overlap have achieved widths less than 100 psec, but large-scale systems with this class of resolution may never be sufficiently stable, and will consume enormous amounts of electrical power.

## 4. ENERGY FLOW

### 4.1 General comments

The use of calorimetry will become increasingly competitive and in the majority of circumstances will be superior to magnetic spectrometry in the TeV regime. The depth of the calorimeter needs to grow only logarithmically with energy, and the energy resolution may follow  $E^{-1/2}$  until limited by systematics. These well known facts are summarized in Fig. 9, which compares a rather powerful set of magnetic spectrometers to the expected performance of calorimeters.

A detailed study of hodoscope calorimeters for experiments in the 10 TeV range has been presented to working group VIII by Prokoshkin and is included as a separate report in these proceedings. In that report the characteristics of both photon and hadron calorimeters are discussed, and some examples for specific experiments are developed. The remainder of this section addresses the possibilities for a multi-TeV spectrometer designed for the highest rate environment.

#### 4.2 A full solid angle spectrometer for a luminosity above $3 \times 10^{33} \text{ cm}^{-2} \text{ sec}^{-1}$

Present techniques allow the construction of spectrometers capable of handling luminosities of about  $3 \times 10^{32}$  for pp or  $\bar{p}p$  collisions (the nondiffractive cross-section is about 33 mb). The ordinary scintillators used in such devices give pulses of  $\approx 30$  nsec with further tails, comparable to the resolution of MWPC's. Drift chamber confusion times are more like 100 nsec, and need redundancy to approach comparable time resolution. We seek to show here examples of techniques which would allow an increase in rate capability of an order of magnitude.

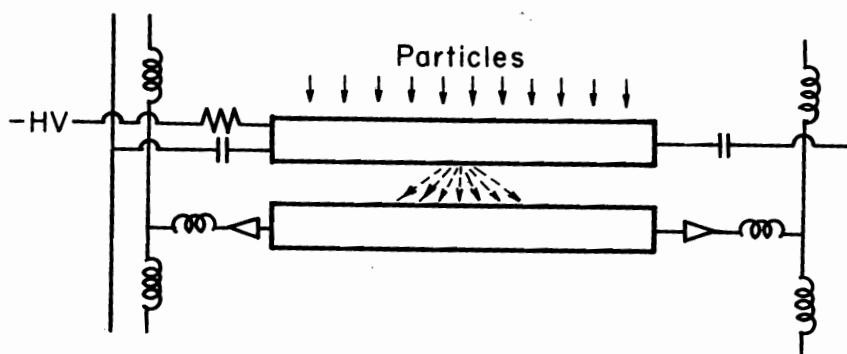
Our strategy here is to consider first the hardest part of the problem: how to deal with small angle particles, those near the incident beam. Most events have particles carrying a major fraction of the energy in a very small angular region, so that spatial subdivision cannot help much. The time resolution simply has to be good enough. For studying high  $p_T$  and high mass states, the most crucial forward detectors are the calorimeters, and we will tackle them first.

We may take as a "standard" calorimeter module the type used in ISR experiment R807: towers of uranium plates about 20 cm square, interleaved with acrylic scintillator, read out by wavelength shifter plates 80 cm long on two sides, leading to photomultiplier tubes at the back. The natural pulse length of such a system is 30-40 ns, determined by the decay times of the fluors. One may search for faster dyes, but there is no assurance of a much faster system. The pulse shape has been measured to be the same for electrons and hadrons, and thus one may consider special shaping networks which cancel the tails of the pulses, and give widths comparable to the rise time of the pulses, about 5-10 ns. This shaping will greatly increase the photon fluctuation noise, but this should not matter for energies of 0.1-10 TeV. Another problem is time jitter caused by longitudinal fluctuations in the hadron shower. The particles have  $v = c$ , and while the light is travelling in the same direction, it has  $v \sim 0.6 c$ . Over the depth of the calorimeter (up to 1.5 m at 10 TeV) this leads to a jitter of  $\pm 0.6$  ns. It can be reduced by more longitudinal subdivision of the read out, but this is not convenient beyond a certain point. It is also hard to hold the time calibration of a large PMT system much better than  $\pm 0.3$  ns.

Thus we may envision an advanced calorimeter system with pulse widths of  $\sim 5$  ns and pulse jitter of  $\sim 0.3$  ns. This will allow  $L \sim 10^{33}$ , but is not quite to our goal. Also, an optical system made of plastic is quite sensitive to radiation damage, appearing first as lowered light output, then as increased attenuation length. One may use replaceable liquid scintillator, but transparent materials must be used to separate the scintillator and wavelength shifter.

Let us consider a purely electrical system. The relatively large signals from high energy particles allow very fast circuitry to be used. The signals will come from the motion of free ionization electrons in a fluid between the metal plates of the calorimeter. The signal current is proportional to the drift velocity of the electrons. This is highest in organic fluids in strong fields. We wish this pulse to be very short, say 1 ns. This may be accomplished by poisoning the fluid with electro-negative materials so that the electron lifetime is  $\sim 1$  ns. The lifetime should not be shorter, because the integrated signal will decrease excessively. What fluid should be used? Room temperature organic liquids may be quite convenient. They have been shown to have electron lifetimes of more than 1000 ns when very carefully purified. The practicality of obtaining the purity corresponding to 1 ns needs to be checked. Collision frequency arguments suggest that it might not be too difficult.

The next problem is to devise a calorimeter structure which also looks like a transmission line up to several GHz. A suggestion for one individual gap is shown in cross section in Fig. 10.



XBL803-3177

Fig. 10. Electrical arrangement needed for each gap of high luminosity calorimeter using liquids with  $\approx 1$  nsec lifetime for free electrons.

The plate thickness might be about 10 mm. The expected energy resolution for 10 TeV is then about 0.4%. The plates are in the form of strips about 10 to 50 mm wide and 200-400 mm long. There is a preamplifier at each end of the plate, terminating the transmission line formed by the plates ( $Z_0 \sim 50$  ohms). The half-width of the plate corresponds to 0.1 ns transit time, and would be consistent with a 0.5 ns rise time for an arbitrary transverse position of the incident ionization (which we suppose to be carried largely in a rather narrow core of the developing shower). It is convenient if the plate is uranium, since the short diffusion length keeps a neutron gas from spreading out over  $\sim 50$  cm as it does in iron. The preamplifier may consist of a Ga-As field effect transistor or fast bipolar, and a line driver. It is coupled to the output line through a

small delay (~1 ns) which compensates for the difference in the velocity in the transmission line and the velocity of light. The system resembles a distributed amplifier. The jitter due to longitudinal shower fluctuations should be limited to a few percent of these compensating delays, or about 30 ps. There is of course a variation in time according to the position along the plate, and for this reason both ends are read out. The mean time determined from the two should be good to a few percent of the full width, again about 30 ps. Events with centroids near the corners of the plates can be off by up to 80 ps, but that affects only a small fraction of all events. It should be possible to obtain an average timing accuracy of about 50 ps. The time difference in the outputs of the two lines gives the transverse position, with an accuracy of about 10 mm. In the direction across the plate, the position is measured by analyzing the shape of the distribution of charge in adjacent strip towers. In the early part of the detector, where the showers are still narrow, one might wish to have widths as narrow as 10 mm.

The high voltage plate must be connected through a bypass capacitor which is part of the output line. One can imagine a ceramic block capacitor running along the edge of the plate. A gap of about 4 mm would be desirable to give enough signal and keep the capacitance low. The high voltage should be as large as possible to keep the drift velocity large, probably 20 to 40 kV. There might be three longitudinal subdivisions, say 0 to 6 radiation lengths, 6 to 18, and the remainder. This would separate electromagnetic particles, and improve spatial resolution.

The treatment of the signals emerging from the detector must be handled carefully. Cables which preserve this kind of pulse length are not simple to find or to use, yet some delay element must be introduced.

With this device, pulse shape analysis will eliminate accidental pile up with time differences greater than 50 ps, so that accidentals could be reduced to a fraction of a percent with this information alone. Other requirements will reduce accidentals further. For example, the timing of the forward calorimeters will fix the longitudinal position of the interaction vertex within a cm. This must agree with the position determined by large angle tracks. Also, the total energy observed in the event, which will usually be near the beam energy, must not be more than the beam energy, within the few percent resolution. The limitation on beam rate is thus probably not accidentals in the final data, but dead time due to rejection of detected accidentals, and concomitant processing time increases. If 1 ns pulses are achieved in the forward calorimeters, the first consideration would allow  $L = 10^{34}$ . Whether this ultra-high rate capability can be realized in a complete spectrometer depends on the other detectors as well, and these are discussed next.

In the very forward direction, tracking might be provided by a secondary emission-charge division detector, a technique with very high

rate capability and under development by Palmer and Rehak et al. at BNL. At large angles, the measurement of curvature in a magnetic field may be attempted using scintillating fibers coupled to avalanche photodiodes (APD) followed by fast low noise FET amplifiers. Strand et al. at BNL have successfully detected single particles with such an arrangement. The APD's have  $\approx 1$  nsec pulse capability, and to preserve the needed performance the very latest FET technology must be employed (hopefully commonplace when TeV machines are in operation). Each end of the fiber (oriented parallel to the magnetic field) is connected to an APD, which are unaffected by the magnetic field but must be protected from high radiation zones. There must be  $10^4$  fibers of  $\approx 1.5$  mm diameter, some of which may have to be replaced about twice a year owing to radiation damage.

Transition radiation detectors of the type discussed earlier in this report, drift chambers and more conventional calorimeters can complete the wide-angle array of detectors since the rates here are relatively low.

This device may be applied to pp,  $p\bar{p}$  storage rings, as well as to hadron or muon beams from a fixed target accelerator. It indicates that cross sections of  $10^{-40}$  cm<sup>2</sup> can be measured in an open, full solid angle detector.

#### 5. NEW DATA ACQUISITION ARCHITECTURE

Here the possibilities for future developments appear especially rich and diverse, and few limitations are foreseen. As noted earlier, advances are less likely to appear as sweeping improvements in front-end time resolution than as consequences of the rapid and continuing evolution in digital technology used in multi-level triggers and preprocessing. The very high multiplicities characteristic of both proton and electron machines make detector techniques which generate 3-dimensional space points particularly worth developing. Extensive parallelism in preprocessing will be more evident as the costs of specialized, dedicated hardware become less of an obstacle. The traditional role of computing centres will change, with less emphasis on big mainframe numbercrunchers, and more on data base management and interactive, even 3-dimensional graphics. The costs of software development, already greater than hardware costs, will continue to rise. World-wide data transmission networks employing wideband communication satellites may be in practice, allowing remote institutes to have close contact, even a "control room" atmosphere.

The electron-positron collider should not present any special difficulties in the triggering, processing data acquisition or recording. The use of calorimetry will provide a powerful means of rejecting most of the background. Depending on the arrangement, a typical hadronic event might involve 40-80 kbytes of data, and trigger

rates of 10 Hz could be tolerated. The experience with LEP should offer a nearly direct basis for planning the  $\sqrt{s} = 700$  GeV data acquisition systems.

The hadronic machines will present a much more demanding environment for low cross-section studies. Regrettably, there was insufficient time to study the varied data acquisition problems of this class of experiments. We would recommend that future workshops study in detail some experiments aimed at interesting low cross-section reactions, in a data acquisition environment now being formed, namely FASTBUS. This system even if generally adopted will still take several years to mature, and could be the backbone of future developments needed for multi-TeV physics.

## 6. CONCLUSIONS

The possibilities for the advancement of detection and measurement techniques appear rich and diverse, with few limitations foreseen in principle for the experiments done with these machines. However, significant effort is necessary to realize these prospects. The effort will be an excellent investment for the advancement of physics.

\* \* \*

## REFERENCES

- 1) B. Cork and T. F. Hoang, LBL-9950 and references therein.
- 2) J. Seguinot and T. Ypsilantis, Nucl. Instr. and Meth. 142, 377 (1977).
- 3) C. Fabjan, "Detectors for LEP: Methods and Techniques", Proceedings of the LEP Summer Study, CERN PUB 79-01, Vol. II, pp. 716-718.
- 4) M. Benot, J. C. Bertrand, A. Maurer and R. Meunier, CERN-EP/79-51 or Nucl. Instr. and Meth. 165, 439 (1979).
- 5) A. H. Walenta, J. Fischer, H. Okuno, and C. L. Wang, Nucl. Instr. and Meth. 161, 45 (1979).
- 6) P. Rehak and A. H. Walenta, BNL 26862 (1979).
- 7) F. Sauli, Nucl. Instr. and Meth. 156, 147 (1978).
- 8) R. W. Crompton and L. G. H. Huxley, The Diffusion and Drift of Electrons in Gases, New York, John Wiley & Son, 1974.
- 9) B. Sadoulet and V. Palladino, Nucl. Instr. and Meth. 128, 323 (1975).
- 10) B. Dolgoshein and I. Golutvin, private communication to working group VIII.
- 11) B. Dolgoshein, I. Golutvin, and V. Kaftanov, *ibid.*
- 12) K. Lanius, *ibid.*
- 13) M. Miyajima et al., Nucl. Instr. and Meth. 160, 239 (1979).
- 14) W. Willis, private communication to working group VIII.